

A Study of the Influence of LiI on the Chain Conformations of Poly(ethylene oxide) in the Melt by Small-Angle Neutron Scattering and Molecular Dynamics Simulations

B. K. Annis* and Man-Ho Kim

Chemical and Analytical Sciences Division, Oak Ridge National Laboratory, P.O. Box 2008, Oak Ridge, Tennessee 37831-6197

George D. Wignall

Solid State Division, Oak Ridge National Laboratory, P.O. Box 2008, Oak Ridge, Tennessee 37831-6393

Oleg Borodin and Grant D. Smith

Department of Chemical and Fuels Engineering and Department of Materials Science and Engineering, 122 S. Central Campus Dr., Rm 304, University of Utah, Salt Lake City, Utah 84112-0560

Received March 13, 2000; Revised Manuscript Received July 17, 2000

ABSTRACT: Small-angle neutron scattering (SANS) experiments and molecular dynamics (MD) simulations have been performed on poly(ethylene oxide)/LiI solutions at a salt concentration corresponding to ether oxygen:Li = 15:1. Both SANS measurements and simulations revealed a substantial reduction (10–15%) in the radius of gyration of PEO chains in the PEO/LiI solutions compared to chains in the pure melt. The characteristic ratio of PEO chains in the melt as obtained from simulations compared well with the values from SANS experiments. Detailed analysis of the MD trajectories revealed a broad distribution in the number of ether oxygen atoms per 12 repeat unit chain involved in Li⁺ cation complexation, with a strong preference for zero, three, and six ether oxygen atoms per chain. Chains not directly involved in cation complexation (zero complexing ether oxygen atoms) were found to have chain dimensions similar to those in the pure melt. Chains with one to three ether oxygen atoms involved in cation complexation actually showed an increase in radius of gyration. Chains with four or more ether oxygen atoms involved in cation complexation showed increasingly narrow radius of gyration distributions and decreasing radius of gyration, reflecting tight wrapping of the chains around the Li⁺ cations.

Introduction

Polymers such as poly(ethylene oxide) (PEO) and poly(propylene oxide) are able to dissolve alkali salts, thus forming polymer electrolytes, a new class of ionically conducting materials. These materials combine good overall performance with ease of fabrication, light weight, and environmental safety, positioning them among the best candidates for lithium ion and lithium metal secondary batteries.¹ However, their low room-temperature conductivity and low cation transport number limit secondary cell performance, hindering widespread practical applications. Despite significant recent progress in understanding macroscopic and microscopic properties of polymer electrolytes, a detailed picture of the property/structure relationships in these materials is still lacking. In an attempt to improve this picture, we have undertaken a series of combined molecular dynamics (MD) and the experimental studies of PEO/LiI solutions. In our previous papers, we developed a quantum chemistry based force field^{2–3} and performed MD simulations of PEO/LiI solutions^{4–6} focusing on the effect of salt on local polymer conformations, polymer dynamics, and mechanisms of cation transport. Particularly, neutron scattering isotopic substitution (NDIS) experiments together with MD simulations performed on PEO/LiI provided detailed information about the Li⁺ cation environment and demonstrated the ability of the MD simulations to accurately represent the polymer/salt interactions.⁶ In this work, we focus

our attention on the effect of LiI salt on global polymer conformations reflected by the radius of gyration of the PEO chain.

Numerous Raman and infrared spectroscopic studies,^{7–10} and MD simulations of amorphous PEO and its low molecular weight oligomers containing lithium and sodium salts^{11–13} indicate that polymer conformations change with addition of salt. These studies, along with our own simulation studies,⁴ indicate an increase in the gauche population of the C–C dihedrals with increasing salt concentration. Such changes in local conformations may lead to changes in overall chain dimensions. For example, intrinsic viscosity measurements in salt-containing aqueous solutions of PEO¹⁴ have indicated that salt reduces the coil dimensions in an aqueous environment. Unfortunately, absolute conformer populations cannot be obtained from Raman and infrared spectroscopic measurements, thus making the quantitative comparison with MD simulations predictions difficult. However, SANS experiments can provide quantitative information about changes of the global chain conformations as a function of salt concentration by means of the mean-square radius of gyration. R_g , given as the root of the measured (mean-square) value, can be directly compared with the results of MD simulations performed on the same system. Below we present such a comparison for the PEO/LiI solution at 361 K and the salt concentration corresponding to ether oxygen:Li = 15:1.

Experiment

The fully deuterated and protonated forms of PEO of the structure $\text{CH}_3\text{--CH}_2\text{--O--}(\text{--CH}_2\text{--CH}_2\text{--O--})_n\text{--CH}_2\text{--CH}_2\text{--OH}$ were prepared by anionic polymerization by Polymer Source, Inc. The molecular weight distributions were obtained from size exclusion chromatography. The polydispersities of both the H and D polymers were found to be 1.04 with $M_{\text{wD}} = 26.7$ kg/mol and $M_{\text{wH}} = 23.2$ kg/mol. The molecular weight values include the mass difference between the H^1 - and D^2 -labeled segments and must therefore be divided by 44 and 48, respectively, to give the degrees of polymerization $N_{\text{wH}} = 527$ and $N_{\text{wD}} = 556$ ($N_{\text{rH}} = 506$, $N_{\text{rD}} = 534$). The lithium iodide (LiI) had a purity of 99% and was obtained from Aldrich. Five D-PEO/H-PEO mixtures with molar ratios 0/100, 10/90, 30/70, 50/50, and 100/0 were prepared by dissolution in HPLC grade acetonitrile at 65 °C. LiI was also dissolved in acetonitrile and added to the polymer solutions to give a 15:1 ratio of ether oxygen atoms to LiI. These procedures were carried out in a drybox, and the final solutions were dried in a vacuum oven. The resulting films were inserted in quartz cells and alternately evacuated and pressurized at ~80 °C to remove bubbles. When the samples were optically homogeneous, the temperature was increased to ~100 °C for about 1 h before transference to the SANS furnace which was held at ~90 °C under an inert atmosphere.

The SANS data were collected on the W. C. Koehler SANS facility¹⁵ at Oak Ridge National Laboratory. The coherent intensities were obtained by applying standard empirical corrections¹⁶ for incoherent background and void contributions. Net intensities were converted to an absolute ($\pm 4\%$) differential cross section per unit sample volume (in units of cm^{-1}) by comparison with precalibrated standards.¹⁷

Analysis

The experimental data were treated in two ways, both of which make use of the random phase approximation^{18,19} (RPA) in the form for polydisperse chains^{18,20} which makes allowance for the slight difference in the degrees of polymerization and small polydispersities. In this case the coherent scattering intensity in cm^{-1} is given by

$$I(Q) = \frac{(a_{\text{D}} - a_{\text{H}})^2}{v} \{ [\phi_{\text{D}} N_{\text{D}} g(x_{\text{D}})]^{-1} + [(1 - \phi_{\text{D}}) N_{\text{H}} g(x_{\text{H}})]^{-1} \}^{-1} \quad (1)$$

where the volume fraction of deuterated chains is ϕ_{D} , N_{D} and N_{H} are the degrees of polymerization of the deuterated and protonated chains, respectively, v is the monomer volume, a_i is the sum of scattering lengths for a monomer, and g is given by

$$g(x_i) = \frac{2}{x_i^2} \left[x_i - 1 + \left(1 + \frac{x_i}{k_i} \right)^{-k_i} \right] \quad (2)$$

with

$$x_i = (QR_{gi})^2 \quad (3)$$

and

$$k_i = \left(\frac{N_{wi}}{N_{ni}} - 1 \right)^{-1} \quad (4)$$

where R_{gi} is radius of gyration of component i and corresponds to a chain with the number-average degree of polymerization. N_{wi} and N_{ni} are the weight- and number-average degrees of polymerization, respectively.

As both components are from the same species (PEO), the only thermodynamic interaction between the constituents is the isotopic Flory–Huggins parameter (χ_{HD}) between H^1 - and D^2 -labeled segments. To our knowledge, no perturbation of the scattering due to isotopic labeling was observed in previous SANS studies,^{21,22} despite the fact that the molecular weights used were much higher ($M_w \sim 10^5$) than in this work. As such “isotope effects” are generally observed^{23,24} only at higher molecular weights, where $N_{\chi_{\text{HD}}} \sim 1$, they should be even smaller in these studies, and we have therefore assumed that the effect of the isotopic χ parameter is negligible.

If the polydispersities of the H and D chains are the same, application of the RPA, in principle, only requires three parameters, i.e., the degrees of polymerization of the H and D species and a single R_g , since $R_{\text{gD}} = (N_{\text{rD}}/N_{\text{rH}})^{1/2} R_{\text{gH}}$. When treated in this manner, the nonlinear least-squares fit indicates that there are too many parameters to be meaningfully determined; i.e., the system is overparametrized.²⁵ Consequently, the chromatographic results were fully incorporated into the polydisperse RPA which leaves only a single parameter, R_{gH} , to be determined.

In the second method of data treatment, the chromatographic results for the ratio of the number-average degrees of polymerization and the polydispersities were used which leaves two parameters: the radius of gyration and the number-average degree of polymerization of the H species to be fitted.

Molecular Dynamics Simulations

The radius of gyration reflects global polymer conformations, necessitating simulation trajectories on the order of at least one Rouse time order to ensure equilibration and adequate statistics. Simulations required for proper equilibration and sampling of high molecular weight polymer chains are not at present feasible. Consequently, we performed MD simulations on an ensemble of 32 shorter PEO chains having molecular weight $M_w = 0.54$ kg/mol with a structure $(\text{H--}(\text{CH}_2\text{--O--CH}_2)_{12}\text{--H})$, thereby allowing proper equilibration and sampling of the PEO chain radius of gyration. Molecular dynamics simulations were performed on pure PEO and PEO/Li melts at EO:Li = 15:1 salt concentration at 363 and 450 K. Details of the MD simulations are given in refs 4 and 22. Rouse times τ_{R} were found to be 11.5 and 1.03 ns. Simulation trajectories of 9 and 7 ns at 363 and 450 K, respectively, were obtainable after equilibration, thus allowing accurate calculation of the radius of gyration.

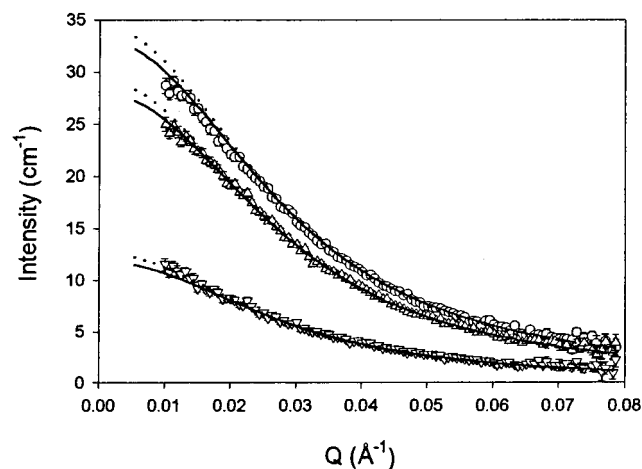
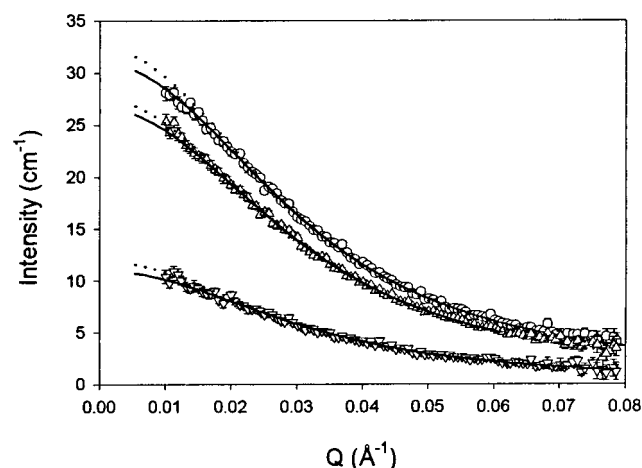
Results and Discussion

The experimental values of the radius of gyration of the pure melt ($R_{\text{g,m}}$) and PEO/LiI solutions ($R_{\text{g,s}}$) from the single-parameter fit as well as the radius of gyration and N_{H} values from the two-parameter fit are given in Table 1. Figures 1 and 2 show the data and the fits for PEO and PEO/LiI melts, respectively. It is clear that the two models deviate somewhat for $Q < 0.02 \text{ \AA}^{-1}$, where the single-parameter model tends to yield systematically higher intensity values. The values of the radius of gyration obtained from the two methods of analysis differ by 4–8%. However, as Table 1 indicates, the ratios of the radius of gyration of the pure PEO to that containing LiI, $R_{\text{g,s}}/R_{\text{g,m}}$, are essentially independent of the method of analysis. The values of N_{H} , the

Table 1. Results of the Single- and Two-Parameter Random Phase Approximation (RPA) for SANS Data Together with the Radius of Gyration Values from the MD Simulations

vol fraction, ϕ_D	single-parameter RPA				two-parameter RPA					
	$R_{g,s}$ (Å)	$R_{g,m}$ (Å)	$R_{g,s}/R_{g,m}$	C_∞ (PEO)	$R_{g,s}$ (Å)	$R_{g,m}$ (Å)	$R_{g,s}/R_{g,m}$	N_H	$N_{H,s}^a$	C_∞ (PEO)
0.50	50.5	54.6	0.92	5.5	48.2	52.5	0.92	485	481	5.3
0.30	50.1	54.8	0.91	5.5	48.5	52.8	0.92	485	488	5.4
0.10	51.6	56.7	0.91	5.9	47.7	52.6	0.91	464	464	5.6
	6.32	7.24	0.87	MD Simulations 5.4 ^b						

^a Monomer volume taken as PEO monomer volume + (1/15) LiI volume. ^b Corrected for the molecular weight difference, see text.

**Figure 1.** PEO at 361 K: \circ , $\phi_D = 0.50$; \triangle , $\phi_D = 0.30$; ∇ , $\phi_D = 0.10$. One par, RPA model (—); two par, RPA model (\cdots).**Figure 2.** PEO/LiI (15:1 EO/Li) at 361 K: \circ , $\phi_D = 0.50$; \triangle , $\phi_D = 0.30$; ∇ , $\phi_D = 0.10$. One par, RPA model (—); two par, RPA model (\cdots).

number-average degree of polymerization of the H species obtained from the two-parameter RPA calculations, are also in reasonable agreement with the value of 506 from the size exclusion chromatography. In the two-parameter fit the monomer volume and N_H are coupled, and in the case of PEO/LiI it was assumed that the average monomer volume was equal to that of PEO and 1/15 of a LiI molecule. As may be seen in Table 1, the N_H values of the pure and salt-containing melts are quite similar and justify this assumption.

Another type of data analysis that can be used which avoids any effects of polydispersity and to a first approximation any dependence on the degrees of polymerization is the use of the so-called Kratky plateau in a plot of $Q^2 I(Q)$ vs Q .¹⁷ The plateau region typically occurs at about $Q = 0.06 \text{ Å}^{-1}$ and is inversely propor-

tional to R_g^2 and the monomer volume.^{17,26} We have estimated the ratio of the plateau values and, in connection with the above-discussed approximation for the monomer volume for PEO/LiI, a value of 0.93 for the ratio of $R_{g,s}/R_{g,m}$ results. This is consistent with the values 0.91–0.92 obtained by the RPA fits, but because of the low scattered intensity, the strong dependence on the estimated incoherent background which amounts to approximately half the total intensity for the D-PEO 10/H-PEO 90 samples and the dependency on the monomer volume ratio, we believe the RPA approach to be more reliable.

Table 1 also includes the values of $R_{g,s}/R_{g,m}$ at 363 K obtained from MD simulations. Reasonable agreement with experiment can be seen. We believe the difference between SANS experiment and MD simulations is within the overlap of the mutual uncertainties. Hence, both simulation and experiment indicate that LiI salt results in a substantial reduction in R_g . Another useful way of comparing dimensions for chains with different degrees of polymerization is through the characteristic ratio, C_∞ .²⁷ For a Gaussian chain this is given by

$$C_\infty = \frac{6R_g^2}{n\ell^2} \quad (5)$$

where ℓ is the mean-square bond length (2.1436 Å^2 for PEO) and n is the total number of skeletal bonds (3 times the degree of polymerization). From Table 1 it can be seen that the two approaches of data analysis give similar values for the characteristic ratios of pure PEO. The experimental results compare reasonably well with the value of 5.7 at 371 K obtained in a recent SANS²² study on PEO with a degree of polymerization of about 2400. These values are also in reasonable agreement with those obtained from MD simulations of the shorter, model chains at 363 K after a rotational isomeric state based molecular weight correction has been made to the latter.²² This agreement indicates that the simulations not only capture the influence of LiI on chain dimensions but also do a credible job in reproducing the actual chain dimensions in pure PEO and PEO/LiI solutions. An earlier SANS study²¹ on PEO which was considerably more polydisperse than that used here and with an average degree of polymerization of about 2500 resulted in a value of C_∞ at 353 K of 6.9, which now appears too large.

Experiments can access the radius of gyration averaged over all the PEO chains. MD simulations allow us to consider the effect of the salt on the polymer dimensions in greater detail. We proceed by investigating the dependence of the PEO radius of gyration on the number of the ether oxygen atoms complexed with a Li^+ cation. An ether oxygen (EO) atom was considered to

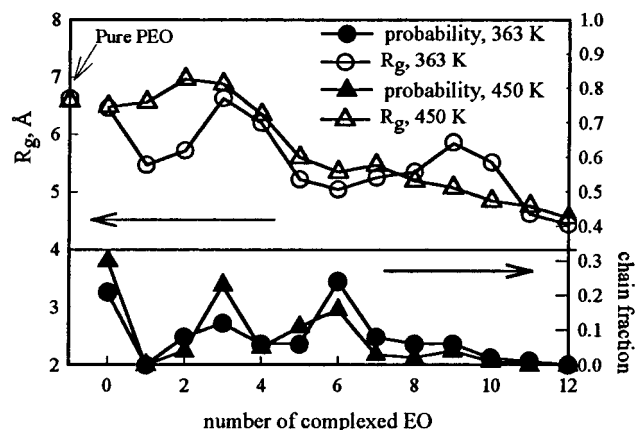


Figure 3. Radius of gyration (R_g) and probability of PEO chain having a given number of complexed EO for PEO/LiI, EO:Li = 15:1 at 363 and 450 K. The radius of gyration of PEO in the pure PEO melt is also shown for comparison.

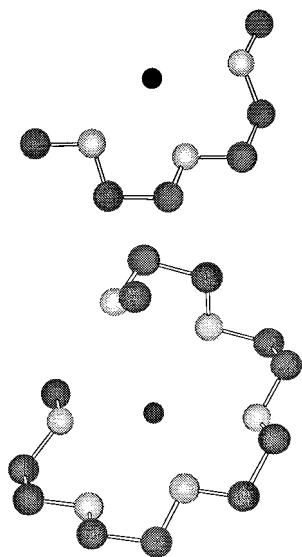


Figure 4. Complexing of Li^+ cation by the three and six ether oxygen sequence of a PEO chain. The most probable complexation sequences *tgt tgt* and *tgt tgttgttgtg* for the EO_3 and EO_6 segments are shown.

be complexed when it had at least one Li^+ cation in its first coordination shell (4.0 Å). The radius of gyration and the fraction of PEO chains having different numbers of complexed EO are shown in Figure 3 at 363 and 450 K, together with the radius of gyration of the pure PEO melt chains. Figure 3 indicates a strong tendency of zero, three, or six EO per chain to be involved with cation complexation. At 450 K, the radius of gyration can be observed to decrease with increasing number of complexed EO beyond three. Chains with one to three ether oxygen atoms involved in cation complexation show an increase in R_g . These effects are due to the geometry of the complexing sequences, as illustrated in Figure 4. The sequence of three complexed EO shows little influence of the cation on the global chain conformation while in the six EO sequence the chain wraps around the cation, resulting in a tight coil geometry. While the poorer statistics at 363 K preclude quantitative interpretation, a trend of decreasing radius of gyration with increasing number of complexed EO can be observed. It is worth noting that the PEO chains in the PEO/LiI solutions not involved with cation complexation have a radius of gyration similar to that of PEO

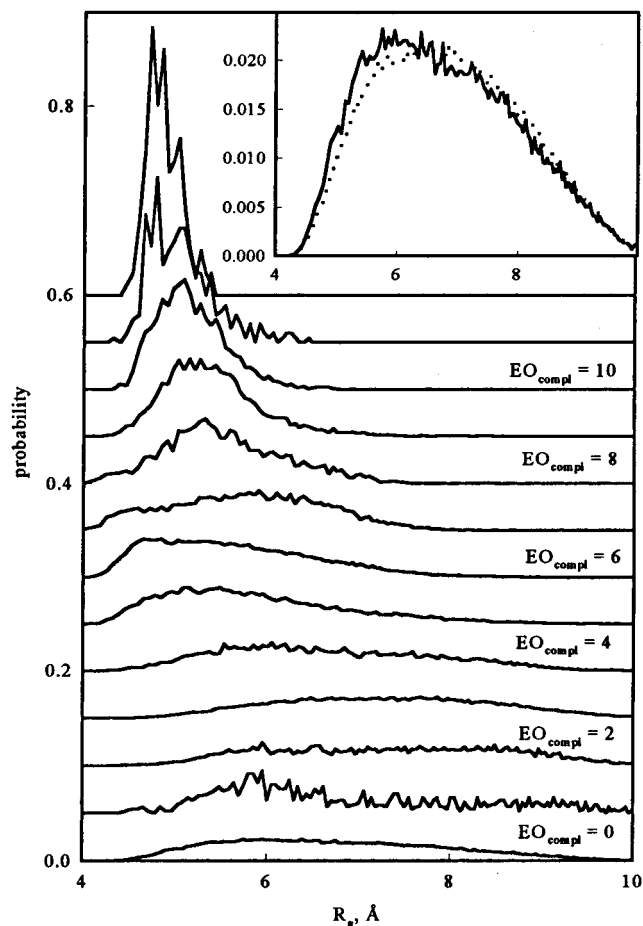


Figure 5. Distribution of the radius of gyration for PEO chains having a given number of complexed EO for PEO/LiI, EO:Li = 15:1 at 450 K. The distributions have been shifted by $n \cdot 0.05$, where n is the number of complexed ether oxygen atoms. The inset shows the radius of gyration distribution for uncomplexed PEO chains in PEO/LiI (solid line) together with that for PEO in the pure PEO melt.

chain in pure PEO melt. This is in agreement with our previous supposition⁶ that PEO/LiI solutions at low concentrations ($\text{EO:Li} \geq 15:1$) are a composite of pure polymer and salt-enriched domains. The estimated scattering contrast for such domains is more than 100 times smaller than the contrast between H and D chains, and for the 10 Å size indicated by the radial distribution function of ref 4 these domains would be unobservable in the study reported here. This is supported by the similarity of the scattering that was observed from pure DPEO and DPEO/LiI.

Simulations revealed that, in addition to the radius of gyration itself, the radius of gyration distribution is strongly influenced by the number of EO involved in cation complexation. Figure 5 demonstrates how the distribution of the radius of gyration depends on the number of complexed EO atoms in the PEO chain for the PEO/LiI solution at 450 K. As with the radius of gyration itself, shown in Figure 3, the most probable radius of gyration increases with EO complexation for one to three EO and then decreases. The decrease in the width of the radius of gyration distribution with increasing number of complexed EO is consistent with the geometrical constraints on chain conformations and dimensions due to wrapping of the PEO chain around a Li^+ cation. Finally, the uncomplexed chains in PEO/LiI solutions have a radius of gyration distribution very

similar to that of the PEO chains of a pure PEO melt, as illustrated in the figure inset.

Conclusions

The characteristic ratio of PEO in pure PEO melt was found to be 5.3–5.9 from SANS and 5.4 from the simulations. Both experiment and simulation demonstrate a decrease in radius of gyration of PEO chains of 10–15% in solutions with EO:Li = 15 due to salt complexation. Those chains in PEO/LiI solutions not directly involved with cation complexation were found to have a similar radius of gyration distribution as PEO chains in the pure melt. This observation is in agreement with our previously proposed view of PEO/LiI systems at low salt concentrations (EO:Li \geq 15:1) being a composite of pure polymer and salt-enriched domains. Those chains with one to three EO involved in Li⁺ complexation actually increase in radius of gyration, while those with four or more decrease, with a corresponding narrowing in radius of gyration distribution.

Acknowledgment. The authors thank one of the referees for the suggestion of considering the Kratky plateau type of analysis. This research was supported in part by the Division of Materials, Office of Basic Energy Sciences, U.S. Department of Energy, at Oak Ridge National Laboratory, managed by Lockheed Martin Energy Research Corp. under Contract DE-AC05-96OR22464, by the National Science Foundation—Division of Materials Research through NSF CAREER award DMR 96-24475, and by the Eveready Battery Company through a gift which allowed continuation of this project.

References and Notes

- (1) Gray, F. M. *Solid Polymer Electrolytes. Fundamentals and Technological Applications*; VCH Publisher: New York, 1991.
- (2) Smith, G. D.; Jaffe, R. L.; Partidge, H. *J. Phys. Chem. A* **1997**, *101*, 1705.
- (3) Smith, G. D.; Jaffe, R. L.; Yoon, D. Y. *J. Phys. Chem.* **1993**, *97*, 12752.
- (4) Borodin, O.; Smith, G. D. *Macromolecules* **1998**, *31*, 8396.
- (5) Borodin, O.; Smith, G. D. *Macromolecules* **2000**, *33*, 2273.
- (6) Londono, J. D.; Annis, B. K.; Habenschuss, A.; Borodin, O.; Smith, G. D.; Turner, J. Z.; Soper, A. K. *Macromolecules* **1997**, *30*, 7151.
- (7) Frech, R.; Huang, W. *Solid State Ionics* **1994**, *72*, 103.
- (8) Huang, W.; Frech, R.; Johansson, P.; Lindgren, J. *Electrochim. Acta* **1995**, *40*, 2147.
- (9) Huang, W.; Frech, R. *Macromolecules* **1995**, *28*, 1246.
- (10) Shashkov, S.; Wartewig, S.; Sander, B.; Tubke, J. *Solid State Ionics* **1996**, *90*, 261.
- (11) Muller-Plather, F. *Acta Polym.* **1994**, *45*, 259.
- (12) Muller-Plather, F.; van Gunsteren, W. F. *J. Chem. Phys.* **1995**, *103*, 4745.
- (13) Neyertz, S.; Brown, D. *J. Chem. Phys.* **1996**, *104*, 3797.
- (14) Bailey, F. E., Jr.; Callard, R. W. *J. Appl. Polym. Sci.* **1959**, *1*, 56.
- (15) Koehler, W. C. *Physica (Utrecht)* **1986**, *137B*, 320.
- (16) Hayashi, H.; Flory, P. J.; Wignall, G. D. *Macromolecules* **1983**, *16*, 1328. Dubner, W. S.; Schultz, J. M.; Wignall, G. D. *J. Appl. Crystallogr.* **1990**, *23*, 469.
- (17) Wignall, G. D.; Bates, F. S. *J. Appl. Crystallogr.* **1987**, *20*, 28.
- (18) de Gennes, P. G. *Scaling Concepts in Polymer Physics*; Cornell University Press: Ithaca, NY, 1979.
- (19) Higgins, J. S.; Benoit, H. C. *Polymers and Neutron Scattering*; Oxford University Press: New York, 1994.
- (20) Boué, F.; Nierlich, M.; Leibler, L. *Polymer* **1982**, *23*, 29.
- (21) Kugler, J.; Fischer, E. W.; Peuscher, M.; Eisenbach, C. D. *Makromol. Chem.* **1983**, *184*, 2325.
- (22) Smith, G. D.; Yoon, D. Y.; Jaffe, R. L.; Colby, R. H.; Krishnamoorti, R.; Fetters, L. J. *Macromolecules* **1996**, *29*, 3462. Smith, G. D.; Bedrov, D.; Borodin, O. *J. Am. Chem. Soc.*, in press.
- (23) Bates, F. S.; Wignall, G. D.; Koehler, W. C. *Phys. Rev. Lett.* **1985**, *55*, 2425.
- (24) Wignall, G. D.; Bates, F. S. *Makromol. Chem.* **1988**, *15*, 105.
- (25) SigmaPlot, SPSS Inc., Chicago, IL, 1997.
- (26) Wignall, G. D.; Ballard, D. G.; Schelten, J. *Eur. Polym. J.* **1974**, *20*, 861.
- (27) Flory, P. J. *Statistical Mechanics of Chain Molecules*; Oxford University Press: New York, 1988.

MA000452W